



Reductive decolorization of acid blue 113 azo dye by nanoscale zero-valent iron and iron-based bimetallic particles

Hung-Yee Shu*, Ming-Chin Chang, Jian-Jun Liu

Institute of Environmental Engineering, Hungkuang University, Taichung 433, Taiwan, Tel. +886 426318652, ext. 1200; email: hyshu@sunrise.hk.edu.tw (H.-Y. Shu), Tel. +886 426318652, ext. 4113; email: chang@sunrise.hk.edu.tw (M.-C. Chang), Tel. +886 426318652, ext. 4123; email: b122751@yahoo.com.tw (J.-J. Liu)

Received 13 March 2015; Accepted 7 June 2015

ABSTRACT

In this study, effectively reductive decolorization of wastewater with synthesized C.I. Acid Blue 113 (AB113) was obtained by nanoscale particles of zero-valent iron (NZVI), bimetallic iron/nickel (nFe/Ni) and iron/zinc (nFe/Zn) which were prepared in the laboratory with large surface area and reductive potential. The particle size was identified less than 100 nm by field emission scanning electron microscope (FESEM) that nickel was homogeneously distributed with iron element by FESEM mapping for nFe/Ni sample. Moreover, the surface areas of bimetallic nanoparticle samples such as nFe/Ni and nFe/Zn were significantly increased than that of NZVI. The effects of experimental variables such as nanoparticle dosage, initial dye concentration, and metal composition on AB113 decolorizing were investigated. From the results, the synthesized AB113 wastewater of high color and total organic carbon (TOC) was successfully reductive decolorized using three iron-based nanoparticle samples. The optimal conditions were obtained the best color removal efficiencies in 30 min while an initial dye concentration of 100 mg l⁻¹ and nFe/Ni dosage of 0.2 g l⁻¹. Besides, a modified pseudo-first-order kinetic equation was developed to describe the color removal efficiency affected by both initial dye concentration and nanoparticle dosage. The higher nanoparticle dosage, the higher color and TOC removal efficiencies were obtained within the nanoparticle dosage of 0.2 g l⁻¹. Furthermore, among three iron-based nanoparticle samples, nFe/Ni preformed the best color and TOC removal as well as durability.

Keywords: Zero-valent iron; Bimetallic; Nanoparticles; Reductive decolorization; Azo dye

1. Introduction

The textile industry export revenue sum contributed 11,820 million US dollars value to the 3.9% of

Taiwan total export revenue in year 2012 [1] that is one of the most important industrial categories in Taiwan. There are more than 250 textile dyeing and processing factories, and these factories employ lots of labors. Meanwhile, large quantities of effluents without proper treatment processes directly or indirectly

*Corresponding author.

Presented at the 7th International Conference on Challenges in Environmental Science and Engineering (CESE 2014) 12–16 October 2014, Johor Bahru, Malaysia

discharged to the nearby water bodies from textile industries resulting serious damage of the ecological environment and threat of human health. The high color and organic concentrations in textile effluents are usually difficult to be degraded and decolorized that the serious impact for water environment has drawn the attention of public and government. Therefore, Taiwan Environmental Protection Agency enforced the National Effluent Standard of textile industry to meet the 550 true color units of American Dye Manufacturers Institute (ADMI) by year 2003 [2] that compelled the industries develop more efficient pretreatment or polishing processes for dealing with high color effluents. Not only in Taiwan, the textile industries of elsewhere all faced the higher and higher pressure from stricter governmental regulations and public attentions. Therefore, the development of textile wastewater treatment technologies to especially solve high color problems has drawn much attention from research communities and industries in this decade [3–10].

Azo dyes are the largest category of commercial dyes used in textile industry. Therefore, many researches presented successful approaches to degrade and decolorize azo dye compounds by various novel technologies [10–13]. The di-azo dye used in this study, C.I. Acid Blue 113, is applied widely in various textile dyeing industries to dye wool, silk, and polyamide fiber from a neutral or acid bath.

Initially, the application of zero-valent iron (ZVI) in the environmental field was introduced to the soil and groundwater remediation by reactive barrel technology. Further development of nanoscale zero-valent iron, i.e. NZVI, environmental technology was conducted rapidly due to the dynamical development of innovative nanotechnology in all scientific areas.

Many literature reported successful applications of NZVI and bimetallic nanoparticles for remediation of contaminated soil and groundwater through dechlorination reaction of chlorinated hydrocarbons. The target contaminants include trichloroethylene, chlorophenols, polychlorinated biphenyls (PCBs), and polycyclic aromatic hydrocarbons (PAH) [14–17] were reported to be degraded. Inorganic contaminants such as nitrate, perchlorate, and heavy metals were also demonstrated to be remedied by NZVI [18–20].

On the other hand, the applications of ZVI and NZVI for azo dye wastewater treatment were also demonstrated by various researchers. The effective decolorization of five azo dyes by ZVI under anaerobic conditions was presented Cao et al. [21], and the results proposed the decolorization is ensured by the cleavage of azo link in the dye molecule. Nam and Tratnyek [22] explored nine azo dyes with a high

observed rate constant of 0.53 min^{-1} for Orange G by ZVI followed by anaerobic biological treatment, to show improvement of biodegradability. Similarly, Chang et al. presented the efficient decolorization of an Acid Black 24 azo dye by ZVI under ambient condition [23]. Furthermore, a study of Acid Black 24 reductive decolorization by using NZVI with higher surface area and reactivity was demonstrated to spend only about 6/1,000 dosage of NZVI in comparison with microscale ZVI [24]. To overcome the release of nanoparticle problem, Shu et al. presented successful decolorization of Acid Blue 113 by ion exchange resin immobilized NZVI [25].

Use of iron-based bimetallic nanoparticles to replace NZVI can enhance the dechlorination efficiency on soil remediation application. In many researches, the use of Pd in bimetallic Pd/Fe nanoparticles was proved to be effective and successfully enhanced the catalytical activity toward mixtures and single PCBs [15,26]. However, the high cost of Pd makes the technology less feasible to real application. Therefore, exploiting cheaper metals may overcome the problem. Barnes et al. reported effective dechlorination of chlorinated aliphatic compounds by iron–nickel bimetallic nanoparticles [27]. For azo dye decolorization, Shu et al. presented successful decolorization of Reactive Black 5 by activated carbon supported iron–nickel bimetallic nanoparticles [1]. The advantages of NZVI nanotechnology was shown by several papers to be the raising of biodegradability. The applications of NZVI to enhance the efficient bioremediation of PCB-contaminated marine sediment from Venice lagoon were reported by Negroni et al. and Zanaroli et al. to conclude the improvement of biodegradability by NZVI [28,29].

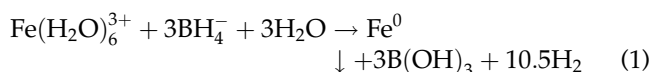
In this study, the reductive decolorization of azo dye C.I. Acid Blue 113 (AB113) using NZVI, iron/nickel (nFe/Ni), and iron/zinc (nFe/Zn) bimetallic nanoparticles was investigated. Operating parameters such as iron/nickel (or iron/zinc) composition, nanoparticle dosage, initial dye concentration, and durability were investigated. The comparison of three iron-based nanoparticle samples, i.e. NZVI, nFe/Ni, and nFe/Zn, was presented on their AB113 degradation efficiencies and total organic carbon (TOC) removal efficiencies. The aim of this study was to present the strong reductive decolorization capability of iron-based nanoparticles and to verify the optimal operating parameters to be applied for efficient treatment of Acid Blue 113 dye. Meanwhile, the protection of zero-valent iron by the second metal element such as nickel and zinc is also important to be revealed.

2. Materials and methods

2.1. Materials and apparatus

The chemical structure of the dye C.I. Acid Blue 113 (C.I. 26,360, $C_{32}H_{21}N_5Na_2O_6S_2$, molecular weight 681.7, characteristic wavelength 566 nm, AB113) is shown in Fig. 1. The dye was obtained from Sigma-Aldrich, Inc., with no further purification for use. Chemicals in reagent grade such as iron chloride ($FeCl_3$), nickel chloride ($NiCl_2$), zinc chloride, and sodium borohydride ($NaBH_4$) were all purchased from Merck & Co., Inc.

Nanoscale zero-valent iron (NZVI), iron/nickel (nFe/Ni), and iron/zinc bimetallic particles (nFe/Zn) were prepared by reductive chemical synthesis in laboratory. The iron chloride ($FeCl_3 \cdot 6H_2O$) solution of 162.2 g l^{-1} mixed with or without appreciate concentration of nickel chloride (or zinc chloride) binary solution was gradually dropped into the sodium borohydride ($NaBH_4$) solution of 30.3 g l^{-1} in a beaker with 10,000 rpm high-speed stirring using a homogenizer. The ferric iron (Fe^{3+}) and nickel (or zinc) ions were reduced to zero-valent iron (Fe^0) and nickel (or zinc) simultaneously and precipitated in nanoscale followed reaction equation as below (nickel or zinc ions follow same mechanism to form nickel or zinc zero-valent precipitation).



After synthesis, the nanoparticles (NZVI, nFe/Ni, and nFe/Zn) suspended in the reaction solution which requires further magnetic collection and residual

reagent washing out. The nanoparticles were collected and washed with deionized water for three times in order to remove the residual reagent followed solid-liquid separation. The above method was modified from a previous study [24]. By solvent exchange with ethanol and evaporation, dry nanoparticles were characterized and identified morphology and sizes in nanoscale (<100 nm) by a JEOL 6330CF field emission scanning electron microscope (FESEM) shown in Fig. 2. Meanwhile, the particle size distribution and BET surface area were obtained within 50–80 nm using a 90 plus particle size analyzer with particle sizing software (Brookhaven Instruments Co.) and specific surface area of $87.87\text{--}145.83 \text{ m}^2 \text{ g}^{-1}$ by the Quantachrome autosorb automated gas sorption system, respectively, as shown in Table 1. Although three nanoparticle samples were formed without pores, pore size and pore volume can be measured by Quantachrome gas sorption system due to the aggregation behavior of nanoparticles. Therefore, pore size and pore volume values are reported in Table 1 as well as specific surface area for reference to compare with other nanoparticles.

2.2. Experimental procedure and analysis

The NZVI, nFe/Ni, and nFe/Zn nanoparticle samples were initially prepared by various concentration compositions of iron chloride, nickel chloride (or zinc chloride) binary solution to obtain various nanoscale iron and nickel (or zinc) loadings. Designated $0.025\text{--}0.2 \text{ g l}^{-1}$ of iron-based nanoparticles was placed in the one-liter batch reactor. The amount (in mg unit) of dye AB113 was precisely measured to dissolve into

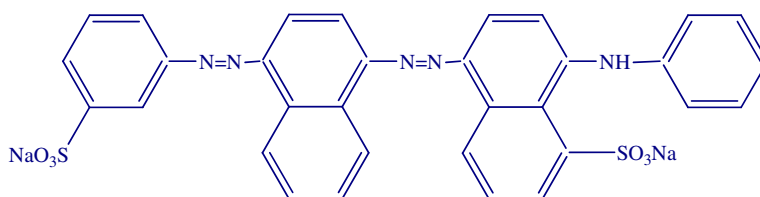


Fig. 1. The chemical structure of the C.I. Acid Blue 113 azo dye.

Table 1
Properties of three iron-based nanoparticle samples

	Specific surface area ($\text{m}^2 \text{ g}^{-1}$)	Pore size (\AA)	Pore volume ($\text{cm}^3 \text{ g}^{-1}$)
NZVI	87.87	12.82	0.026
nFe/Ni	108.38	13.15	0.036
nFe/Zn	145.83	12.97	0.047

one liter of DI water, obtaining a concentration of mg l^{-1} unit. The AB113 dye solution was poured into the reactor, taking into consideration the time, loading of iron-based nanoparticles, initial dye concentration, nickel (or zinc) composition on iron, and durability of nanoparticles at mixing rate of 150 rpm. The reaction runs were performed at ambient temperature of $25 \pm 1^\circ\text{C}$ and unadjusted solution pH of 5.8 ± 0.1 in all cases not investigating effects of temperature and pH.

At defined time intervals, the dye concentration in water samples were withdrawn and measured by a Hitachi U-2000 spectrophotometer with single wavelength absorbance (566 nm) duplicated. The TOC was determined by an IO Analytical 1030W TOC analyzer. The standard color detection procedure developed by the American Dye Manufacturers Institute (ADMI) was employed to evaluate the color intensity of AB113 dye solution. The color intensity was calculated by applying the Adams–Nickerson color difference formula, which substituted transmittance data obtained into 30 wavelengths from 400 to 700 nm in every 10-nm interval, following method 2120E of the Standard Methods. The pH and oxidation reduction potential (ORP) were monitored by a Eutech PH5500 dual channel pH/ion meter with specific probes. The iron nickel and zinc concentrations were measured by a Shimadzu AA-6200 Atomic Absorption Spectrophotometer. Several sets of calibration curves were prepared under various pH conditions (i.e. pH 2,3,6,9, and 11) to reflect the variation of characteristic wavelength and absorbance. And these calibration curves were used to measure the AB113 concentrations under various pH conditions to avoid expected error. In order to test the durability of various iron-based nanoparticles after designed, decolorization experiment was separated from reaction solution by magnetic collection and washed three times by DI water. Then, the recovered iron-based nanoparticles were then applied to a new set of decolorization experiment. The performance of the recovered iron-based nanoparticles was used to evaluate the durability of NZVI, nFe/Ni, and nFe/Zn nanoparticles.

3. Results and discussion

3.1. Characteristics of three iron-based nanoparticle samples

The morphology images (50,000 \times times enlargement) of NZVI before and after reductive decolorization reaction are shown in Fig. 2(a) and (b). The shape of NZVI particles is observed as spherical shape, and the aggregation of particles is formed as a chained-bead shape. After reductive decolorization reaction, the NZVI nanoparticles deform their spherical shape

and aggregate more seriously. And the morphology images of nFe/Ni and nFe/Zn bimetallic nanoparticles are shown in Fig. 2(c) and (d), respectively. The sizes of nFe/Ni and nFe/Zn particles are smaller but the aggregation situations are worse than that of NZVI. In this way, the particle sizes of NZVI, nFe/Ni, and nFe/Zn can be observed to be less than 100 nm from the FESEM images. Furthermore, the iron and nickel (or zinc) amounts in the reaction solution were measured by microwave digestion of NZVI, nFe/Ni, and nFe/Zn nanoparticle samples and analyzed by a Shimadzu AA-6200 Atomic Absorption Spectroscopy. The recovery rates of Fe, Ni, and Zn were determined as 97.5, 90.8, and 91.4%, respectively. From Table 1, the specific surface area of nFe/Zn is the largest of the three types of nanoparticles. In contrast, NZVI is with the smallest specific surface area. From the FESEM–EDS mapping (Fig. 3(a)–(d) for C, O, Fe, and Ni) of nFe/Ni nanoparticle sample, the images present the nickel element on iron particles is uniformly distributed. Similar observation from EDS mapping can be obtained for nFe/Zn (data not shown).

3.2. Decolorization and TOC removal by three iron-based nanoparticle samples

The reaction mechanism of a NZVI reductive degradation system can be explained as follows. In aqueous solution, NZVI produces electrons and ferrous ions by dissolution of NZVI surface. And the dissociated electrons react rapidly with the certain organic compounds (i.e. AB113 in this case) resulting degradation and decolorization. By adding 0.2 g l^{-1} of three iron nanoparticle samples, i.e. NZVI, nFe/Ni (with 50% Ni), and nFe/Zn (with 50% Ni), the AB113 concentration removal efficiencies vs. time are shown in Fig. 4(a). From the figure, AB113 removal efficiencies increase very rapidly and sharply during the first few minutes then remain almost unchanged for rest of reaction time. The AB113 removal efficiencies for three iron-based nanoparticle samples sharply rise to 80.3–95.6% during the first 2 min, promptly increasing to about 96% at 10 min; only less than 3% residual following to 30 min are found in all cases. The removal efficiencies change merely from 10 to 30 min that implies the reductive degradation of AB113 proficiently during initial 10 min, afterward nearly changes for AB113 removal.

The ORP of a solution is a measure of the oxidizing or reduction power of the solution. In an oxidizing environment with presence of an oxidizing reagent, a higher ORP with positive value will exist. On the other hand, a lower ORP presents a more reducing

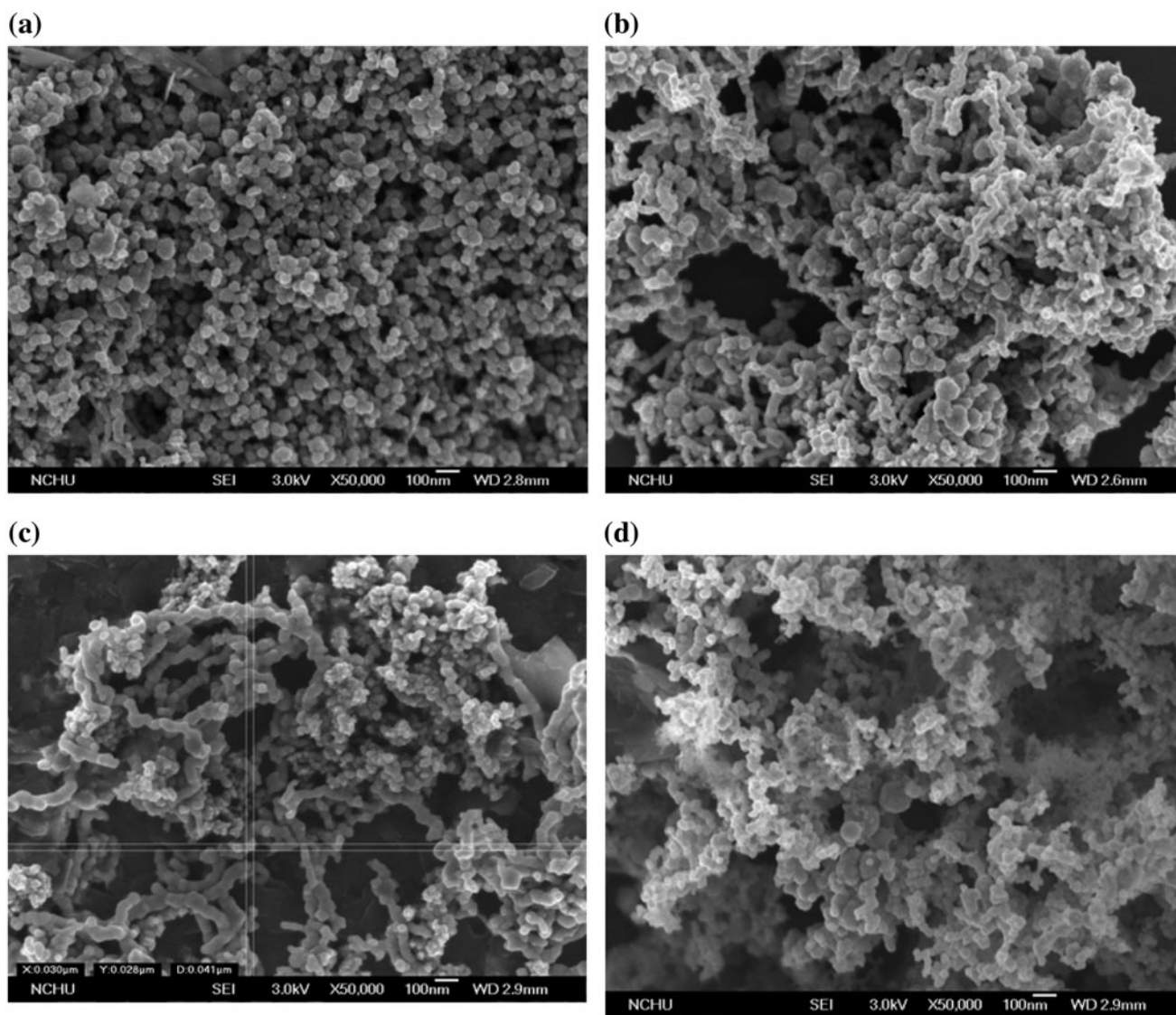


Fig. 2. The morphology images (50,000 \times times enlargement) of NZVI (a) before, (b) after reaction, (c) nFe/Ni, and (d) nFe/Zn.

environment. During this reduction process, the ORP values were detected dropping from 370 mV to lowest points of -421 , -232 , and -391 mV shortly at 15, 15, and 6 min of reaction time for NZVI, nFe/Ni, and nFe/Zn, respectively, as shown in Fig. 4(b). The solution ORP values then increased sharply up to -129 to 91 mV till 30 min. This indicates the reductive condition for effective AB113 removal within the first 10 min. Moreover, the pH variation was also detected during reduction decolorization (Fig. 4(c)), it was first raising sharply from 5.8 to 8.1 during 2 min, then decreasing gradually to 6.2 with time, as soon as the NZVI particles contacted dye solution with initial concentration of 100 mg l^{-1} . Similar pH changes for

nFe/Ni and nFe/Zn bimetallic nanoparticles were observed in designed experimental runs.

Since the reductive reaction by NZVI is not strong enough to break organic bonding, the removal of TOC is mainly by adsorption on to NZVI surface. In a previous study reported that the effective color removal of Orange II resulted from the substantial azo link cleavage to form some intermediate products such as sulfanilic acid and 1-amino-2-naphthol [30]. Similarly, it is highly possible that the azo link cleavage of AB113 by the NZVI particles produce some smaller molecular fragments such as sulfanilic acid and aromatic amines resulting TOC measurement. From Fig. 4(d), the TOC removal efficiency is rather

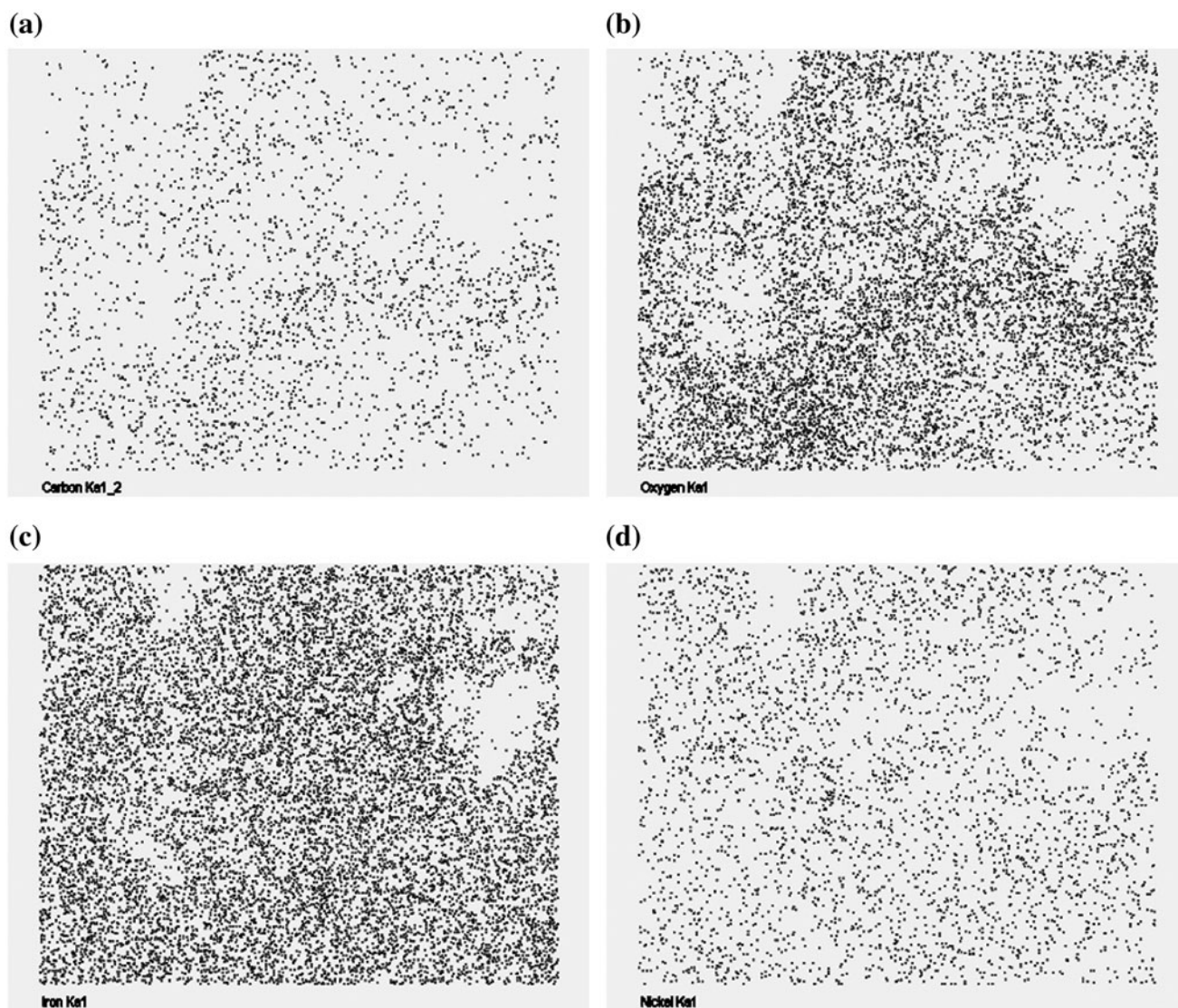


Fig. 3. The FESEM–EDS mapping of elements for nFe/Ni nanoparticles, (a) C, (b) O, (c) Fe, and (d) Ni.

poor for NZVI case, only 33.4% TOC removal was observed at 4 min of reaction time and then dropped gradually to 14.5% in 10 min, later remained small change to 11.7% at 30 min of reaction time. The reason of this observation is that the TOC concentration remained in the solution can be adsorbed through the NZVI particles at the beginning of reaction. Later about 10–15 min, the decrease of TOC removal efficiency is due to the dissolution of iron into the aqueous solution and loss adsorbed organic compounds into aqueous simultaneously. It is interesting to observe that the TOC removal efficiencies for nFe/Ni and nFe/Zn are more effective than that of NZVI. From same figure, the TOC removal efficiencies reach 59.5 and 65.2% for nFe/Ni and nFe/Zn, respectively.

It is fairly good TOC removal in comparison with even oxidation technologies. Under the same condition, it is 96% of the AB113 removal efficiency indicating that TOC reduction is indeed more difficult than color removal. Furthermore, no TOC desorption was presented in these nFe/Ni and nFe/Zn cases. It ensured that the nickel (or zinc) coexist on the iron nanoparticles can prevent dissolution of iron into aqueous solution. On the other hand, the higher specific surface area of nFe/Ni (or nFe/Zn) makes the adsorption more efficient to remove more TOC contribution organic compounds.

Meanwhile, ADMI color index was observed dramatically decreasing from 30,294 to less than 636 for nFe/Ni case. Similar decolorization behavior was also

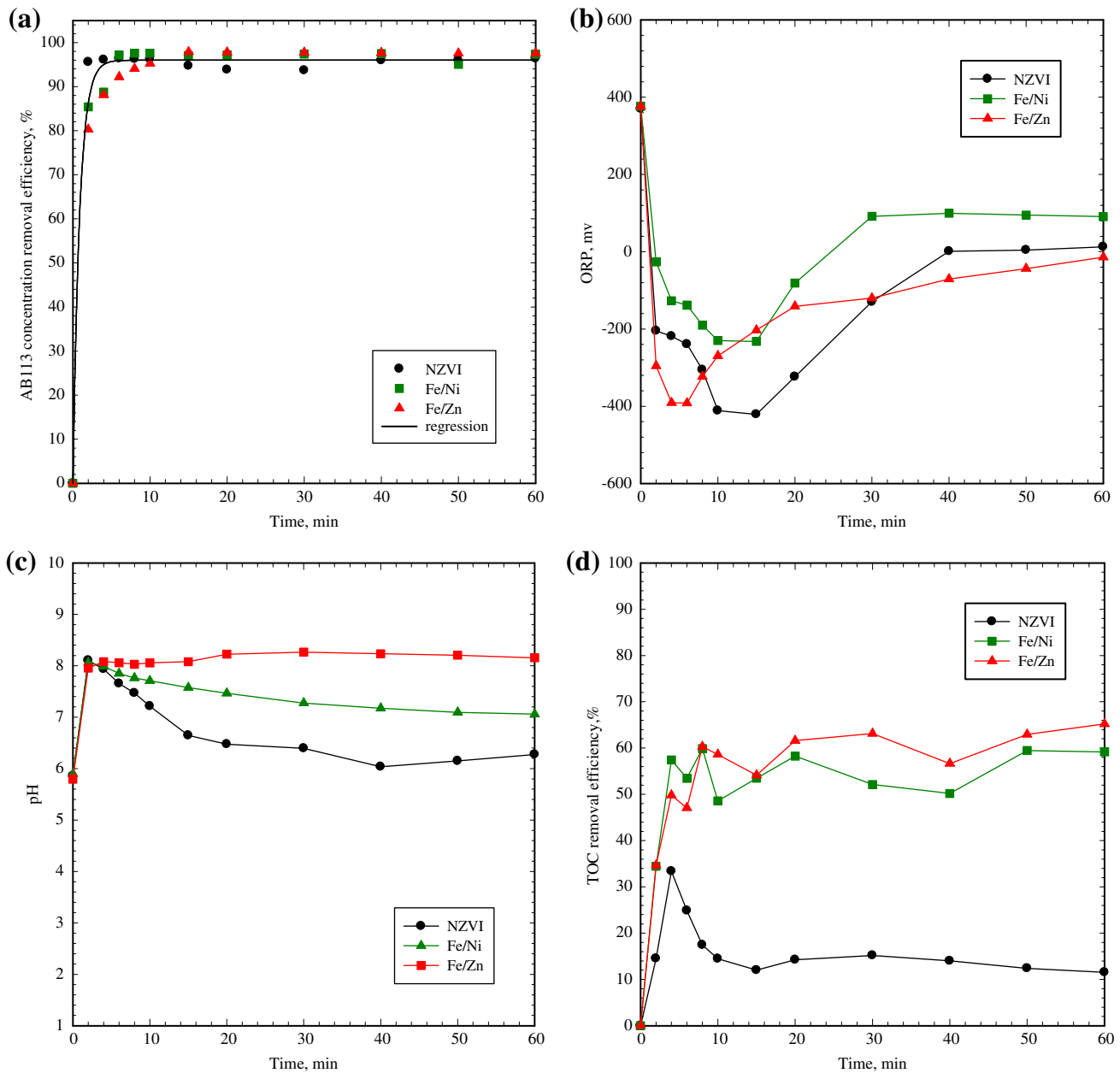


Fig. 4. (a) AB113 removal efficiency, (b) ORP, (c) pH, and (d) TOC vs. time for AB113 reductive decolorization by NZVI, nFe/Ni, and nFe/Zn nanoparticles. (The conditions were initial AB113 concentration of 100 mg l^{-1} , nanoparticle dosage of 0.2 g l^{-1} , nickel or zinc composition of 50%, and reaction time during 60 min.)

obtained for nFe/Zn. However, for NZVI case, due to the dissolution of ferrous ions and further oxidized to ferric ions remained ADMI at about 2,200 level at the end of reaction (data no shown).

For the dye color removal condition, a first-order reaction is generally assumed with respect to dye concentration. It converts into the pseudo-first-order reaction ignoring NZVI particle concentration effect as Eq. (2).

$$C_{\text{dye}} = C_{\text{dye}0} \times e^{-kt} \quad (2)$$

where k denotes the observed first-order reaction rate constant (min^{-1}), t the reaction time (min), $C_{\text{dye}0}$ the initial concentration (mg l^{-1}) of AB113, and C_{dye} is the concentration (mg l^{-1}) of AB113 at time t . The removal efficiency hardly reaches 100% completion due to the limited transfer between water and NZVI particle

interphase so that the residual dye concentration can be expressed by an empirical rate equation proposed in our previous study [24] as Eq. (3).

$$C_{\text{dye}} = C_{\text{ultimate}} + (C_{\text{dye}0} - C_{\text{ultimate}}) \times \alpha \times e^{-kt} \quad (3)$$

where C_{ultimate} is the ultimate residual dye concentration (mg l^{-1}) for certain NZVI dose (g l^{-1}), α denotes the variation coefficient of removed dye concentration for each test, and k denotes empirical rate constant (min^{-1}). The constants of C_{ultimate} , α , and k were obtained by nonlinear regression from Fig. 4(a) resulting C_{ultimate} of 4.013 mg l^{-1} , k of 1.144 min^{-1} with initial dye concentration of 100 mg l^{-1} . Nam and Trantyeck [22] found an observed color removal rate constant of 0.530 and 0.023 min^{-1} for $60 \mu\text{M}$ of Crocein Orange G and $300 \mu\text{M}$ of Naphthol Blue Black G, respectively, by adding 200 g l^{-1} microscale iron. Though the former rate constant was about one half of magnitude comparing with our results, the iron dose demands much differentially that 0.2 g l^{-1} of NZVI, nFe/Ni, and nFe/Zn performed better than the above 200 g l^{-1} of microscale iron. By adding 66.6 g l^{-1} microscale iron, Mu et al. [30] reported the color removal rate constants of Orange II were 0.017 – 0.022 min^{-1} for 0.14 – 0.71 mM . Thus, timely higher color removal and rate constants can be obtained due to the superior surface area of NZVI, nFe/Ni, and nFe/Zn demanding much less dose than that of microscale iron.

On the other hand, during the reaction, the iron concentrations left in solution with time can be reasonably monitored when 0.2 g l^{-1} of NZVI, Fe/Ni, and Fe/Zn nanoparticle samples with 100 mg l^{-1} of initial AB113 concentration. Indeed, the remaining highest iron concentration was 4.4 mg l^{-1} and then precipitated back to the surface of NZVI, Fe/Ni, and Fe/Zn down to 0 mg l^{-1} for longer reaction time. The highest Ni and Zn concentrations during the reaction were measured as 4.43 and 1.89 mg l^{-1} , respectively. The nickel concentration can be decreased down to 0.51 mg l^{-1} at the end of reaction.

3.3. Effect NZVI dosage

As shown in previous studies, the dissolution of ferrous ions and electrons to react with organic molecules on the iron surface and reduction by ZVI in the aqueous phase has been proven to be a fairly fast process [23]. The performance of NZVI follows a mechanism similar to iron dissolution, with the recapture of free ferrous on the NZVI surface to avoid total iron release. The NZVI sample was chosen for dosage

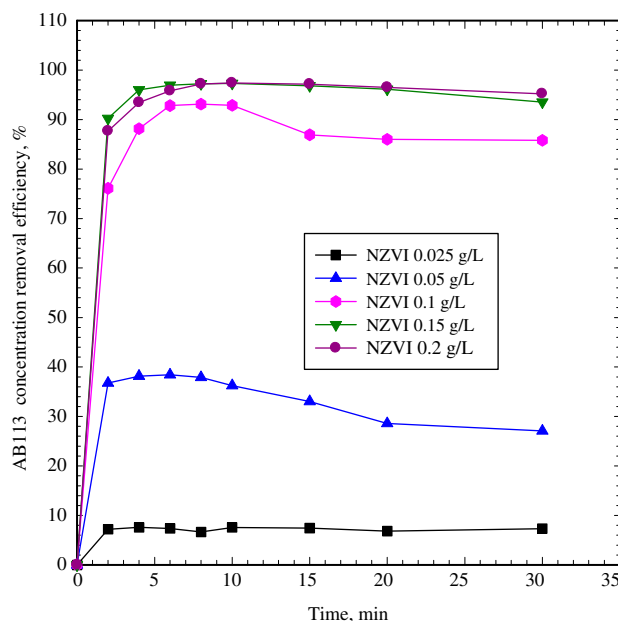


Fig. 5. Effect of NZVI dosage on AB113 removal efficiency. (The conditions were initial AB113 concentration of 100 mg l^{-1} , NZVI dosage of 0.025 – 0.2 g l^{-1} .)

study to represent three iron-based nanoparticle samples. Fig. 5 shows the effect of reaction time on the degradation of AB113 dye with the addition of 0.025 – 0.2 g l^{-1} of NZVI for initial dye concentration of 100 mg l^{-1} . Within the first two minutes, the removal of AB113 concentration was about 7.3 – 90.4% , increasing sharply up to 93 – 96% in 4 min for higher dosage from 0.15 to 0.2 g l^{-1} . For highest dosage of 0.2 g l^{-1} , the AB113 dye concentration quickly dropped down to 2.7 mg l^{-1} and achieved 97.4% removal efficiency during 10 min with the initial concentration of 100 mg l^{-1} . Moreover, no significant change was found until 30 min. This scenario implies that the reductive degradation of AB113 occurs initially within the first 10 min. Afterward, the AB113 concentration removal rarely changes. From the results, pH increased sharply from 6.3 to 8.1 in two minutes and then kept almost unchanged (data not showed). The explanation of pH change in two minutes is according to the mechanism of NZVI dissolution into ferrous ions; spontaneously, the hydroxyl ions are released into the solution and cause the increase of pH. The reductive decolorization of AB113 by NZVI is dominated by the dissolution of ferrous ions and electrons. And the reductive decolorization reaction is happened on the surface of NZVI. Therefore, the higher NZVI dosage provides the more specific surface area and reactive sites to enhance the reductive reaction of AB113 and resulting decolorization of AB113. Similar observation also reported by Shu

et al. [24]. Meanwhile, the dosage effects of nFe/Ni and nFe/Zn are similar to the NZVI case.

3.4. Effect of initial dye concentration

Fig. 6(a)–(c) summarizes the effect of the initial dye concentration on AB113 degradation efficiency by three iron-based nanoparticle samples. In Fig. 6(a), by using

NZVI, the maximum removal efficiency (R_{\max}) declined from 99.5 to 93.4% when initial dye concentration increased from 100 to 800 mg l⁻¹. However, NZVI presented a very good reductive degradation capability on AB113 even with extremely high concentration of 800 mg l⁻¹. This set of experiments ensures that the NZVI is an excellent nanoparticle material for decolorization of azo dyes. Furthermore, the initial rate (r_0)

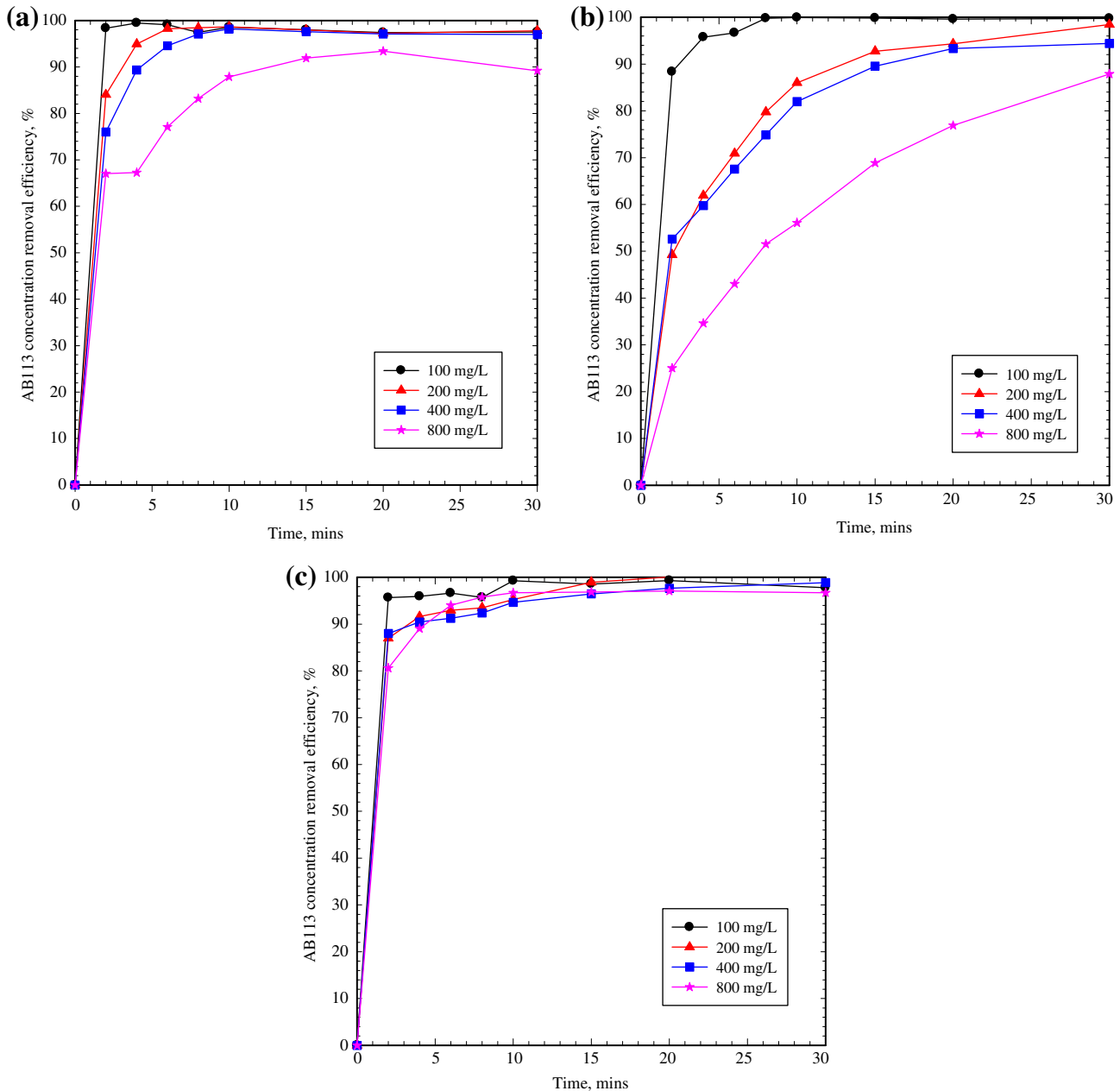


Fig. 6. Effect of initial dye concentration on AB113 removal efficiency by (a) NZVI, (b) nFe/Ni, and (c) nFe/Zn nanoparticles. (The conditions were initial AB113 concentration of 100–800 mg l⁻¹, nanoparticle dosage of 0.2 g l⁻¹, nickel or zinc composition of 50%, and reaction time during 30 min.)

used to evaluate the effect of the initial dye concentration increased from 49.1 to 81.4 and 263.0 mg l^{-1} min^{-1} , with initial AB113 concentration increasing from 100 to 200 and 800 mg l^{-1} , respectively.

By calculation from the results, the unit NZVI-AB113 removal capacity (URC) is the function of the initial AB113 concentration (100–800 mg l^{-1}). Over the course of 30 min, the URCs were 487.44, 946.71,

1878.61, and 3500.07 $\text{mg AB113 per g NZVI}$ with initial dye concentrations of 100, 200, 400, and 800 mg l^{-1} by addition of 0.2 g l^{-1} of NZVI. However, the higher initial concentrations of AB113 obtained the lower dye degradation efficiencies, which provided higher URC at the same NZVI dosage. Thus, it can be concluded that the higher initial AB113 concentration gives the higher URC.

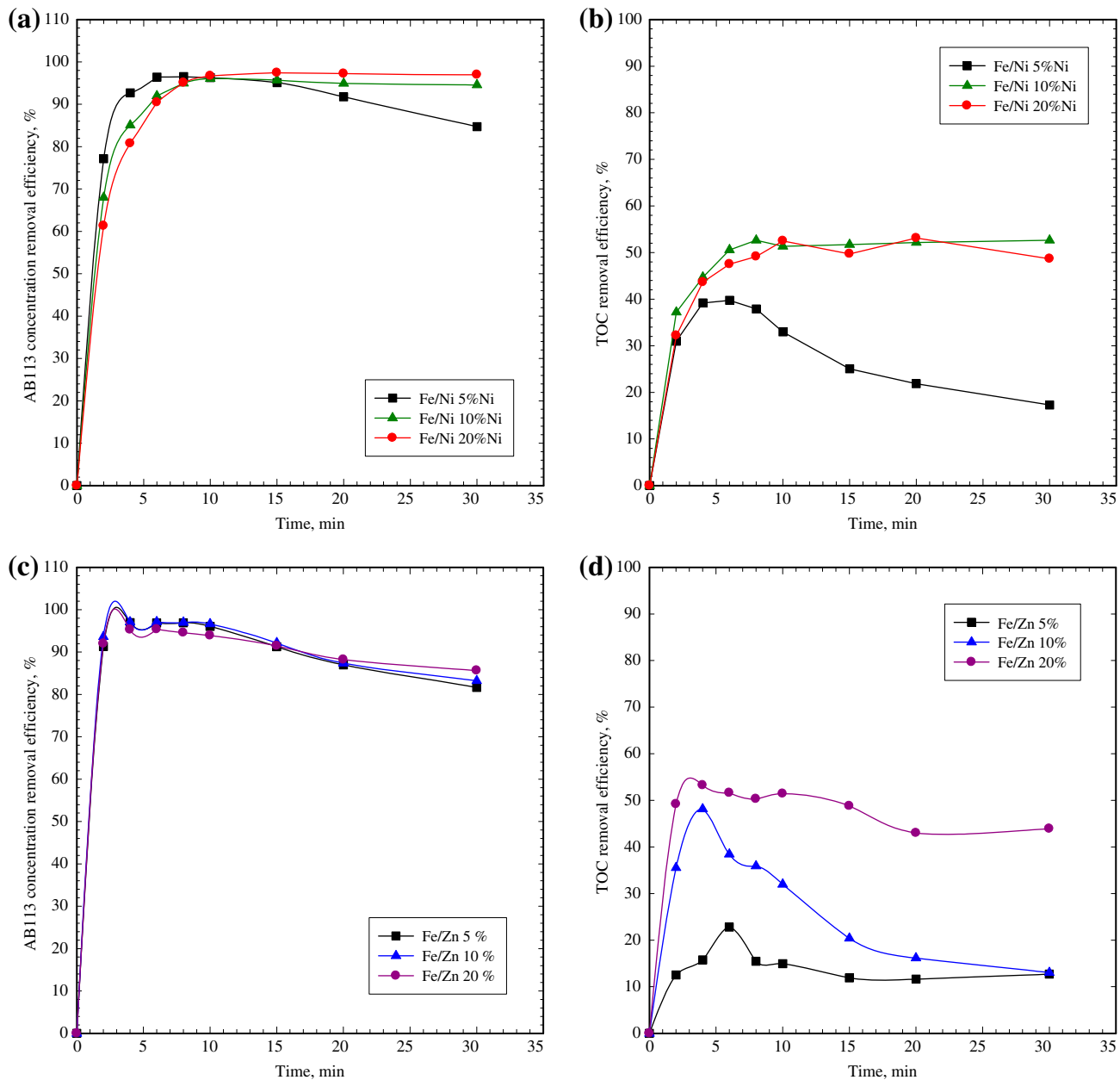


Fig. 7. Effect of nickel composition on (a) AB113 removal efficiency, (b) TOC removal efficiency and effect of zinc composition on (c) AB113 removal efficiency, and (d) TOC removal efficiency by nFe/Ni and nFe/Zn samples. (The conditions were initial AB113 concentration of 100 mg l^{-1} , nanoparticle dosage of 0.2 g l^{-1} , nickel or zinc composition of 5–20%, and reaction time during 30 min.)

From Fig. 6(b), nanoparticle sample of nFe/Ni shows more sensitive effect on initial dye concentration. For the highest AB113 concentration of 800 mg l^{-1} , the removal efficiency reaches only 87.9%. On the other hand, the nFe/Zn presents best capability of decolorizing AB113. In 6 min of reaction time, the removal efficiencies achieve higher than 90% for $100\text{--}800 \text{ mg l}^{-1}$ AB113 concentrations.

The effect of AB113 initial concentration is observed that the highest concentration of 800 mg l^{-1} presents decline of removal efficiency and also initial rate. The reason of this observation is that the higher concentration of AB113 molecules competing for limited NZVI reactive sites, thus, reduces the removal efficiency and initial rate than that of the lower concentration.

3.5. Effect of iron/nickel and iron/zinc compositions

The effect of the iron/nickel composition on AB113 degradation shown in Fig. 7(a) indicates that AB113 degradation initial rate increases with the decrease of the nickel composition on nFe/Ni. For nickel composition from 5 to 20%, the lowest nickel composition of 5% presents the highest decolorization initial rate. However, for higher nickel composition of 10–20% performs stable color removal without dissolution of iron into aqueous solution. Increasing the composition of Ni to 20% can ensure the highest AB113 removal

efficiency till the end of reaction at 30 min. In this case, nFe/Ni with 20%Ni provided substantially more active surface sites and resulting in more nanoscale iron–nickel bimetallic surface collision with more azo dye molecules to enhance AB113 degradation activity.

From the experimental data, the initial AB113 degradation rates of 76.4, 66.9, and $60.0 \text{ mg l}^{-1} \text{ min}^{-1}$ were obtained by the nFe/Ni nickel compositions of 5, 10, and 20% for first 2 min, respectively. Moreover, the final degradation efficiency of AB113 was influenced by nFe/Ni composition. The presence of Ni on nFe/Ni nanoparticles is able to protect nanoscale iron particles from oxidation reaction by dissolved oxygen. And existence of nanoscale iron particles is able to provide high reductive degradation ability. From results, the nFe/Ni with 10–20%Ni compositions performed fairly good AB113 degradation efficiencies of 94.6–97%.

From Fig. 7(b), the TOC removal reached maximum 39.7% removal at 6 min, then, decreased gradually down to 17.3% at 30-min reaction time for nFe/Ni with 5% nickel composition. On the other hand, nFe/Ni with 10–20% nickel composition can present maximum TOC removal of 52.6–53.1% and remain almost unchanged during reaction time of 30 min. The results showed that nFe/Ni bimetallic nanoparticles with higher nickel composition performed better TOC removal capability. On the other hand, for nFe/Zn bimetallic nanoparticles, the

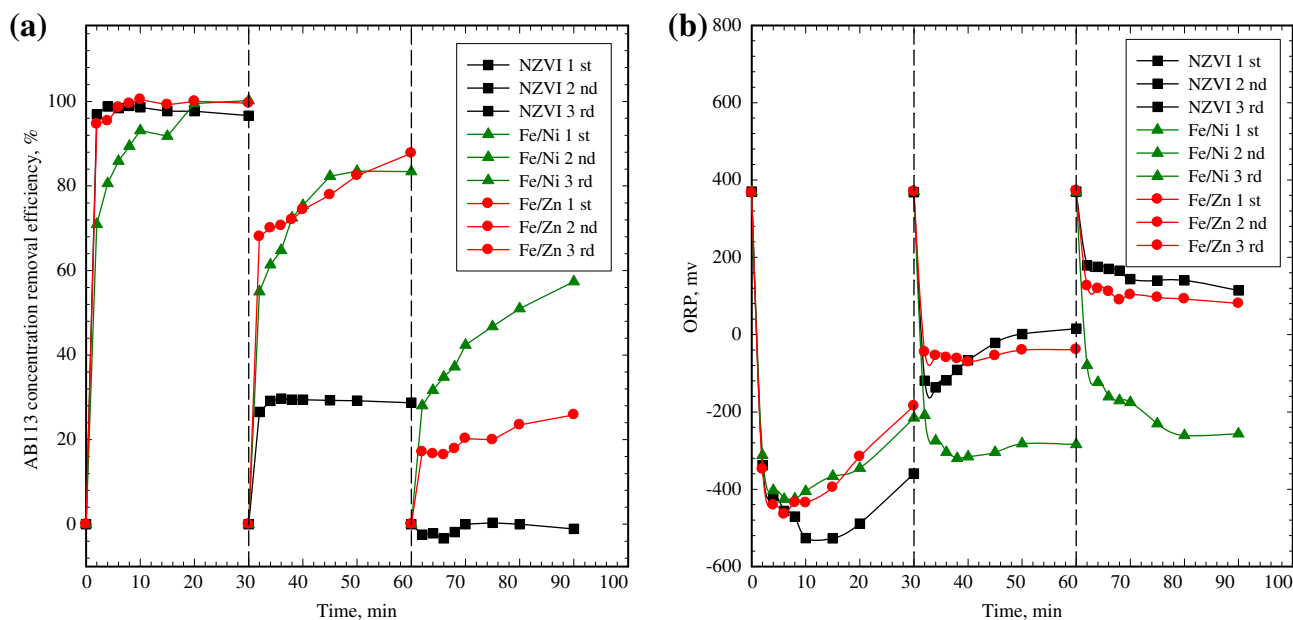


Fig. 8. Durability tests of NZVI, nFe/Ni, and nFe/Zn on AB113 reductive decolorization for three cycles (a) AB113 removal efficiency and (b) ORP. (The conditions were initial AB113 concentration of 100 mg l^{-1} , nanoparticle dosage of 0.2 g l^{-1} , nickel composition of 20% for nFe/Ni and zinc composition of 20% for nFe/Zn, and reaction time during 30 min for each cycle.)

degradation of AB113 (Fig. 7(c)) showed no difference for 5–20% of zinc composition. However, the results in Fig. 7(d) also showed that nFe/Zn bimetallic nanoparticles with higher zinc composition performed better TOC removal capability.

3.6. The durability test

The NZVI, nFe/Ni, and nFe/Zn nanoparticle samples were used repeatedly to treat the AB113 solution. Fig. 8(a) shows the system performance over 3 cycles. Results indicate that the AB113 removal efficiency decays from 97.7% of first use down to 0% at third cycle for NZVI. The nFe/Ni sample shows the best durability of AB113 removal. The final AB113 removal efficiencies decrease from 100, 83.5, to 57.4% for first, second, and third use, respectively. The nFe/Zn nanoparticle sample performs final AB113 removal efficiencies from 100, 87.8, to 25.9% for first, second, and third use, respectively. The results show that bimetallic nanoparticle samples enhance better durability than that of NZVI. The reason for decay in reductive degradation ability is due to the oxidation of NZVI, nFe/Ni, and nFe/Zn bimetallic nanoparticle samples; therefore, the oxidation of nanoparticle samples inhibits the dissolution of iron and electrons into dye solution. The evidence can be observed in Fig. 8(b), as ORP changes during three reuse cycles. For fresh-used nanoparticle samples, the ORP can decrease down to -527, -425, and -464 mV for NZVI, nFe/Ni, and nFe/Zn, respectively. However, when used for the second cycle, the ORP were raised to about -136, -320, and -70 mV for NZVI, nFe/Ni, and nFe/Zn, respectively. For third cycle, only nFe/Ni sample remains in negative ORP status of -261 mV. The results show the loss of reductive reactivity of nFe/Ni is limited and presents best AB113 degradation durability after three decolorization cycles.

4. Conclusions

We have shown that reductive degradation of Acid Blue 113 (AB113) di-azo dye in aqueous solution can be achieved in less than 10 min by adding nanoscale zero-valent iron (NZVI), nanoscale iron/nickel bimetallic particles (nFe/Ni), and nanoscale iron/zinc bimetallic particles (nFe/Zn), under ambient conditions without pH control. After 30 min, more than 96.4–97.9% AB113 concentration and 92.9–99.2% ADMI removal were reached with NZVI (or nFe/Ni and nFe/Zn) dosage of 0.2 g l^{-1} and initial AB113 concentration of 100 mg l^{-1} . In our batch test, the AB113 removal efficiency was dominated by the NZVI dosage

as well as the initial dye concentration. Furthermore, the degradation efficiency increased with increased NZVI load. The nFe/Ni bimetallic nanoparticles presented best AB113 removal efficiency and reuse durability. Accordingly, the results of this study on the effects of NZVI, nFe/Ni, and nFe/Zn nanoparticles dosage, initial dye concentration can be used to optimize the operating parameters of AB113 degradation and provide industries with useful information about this alternative wastewater technology.

Acknowledgments

The authors appreciate the research funding granted by the Taiwan Ministry of Science and Technology (NSC 98-2221-E-241-006-MY3).

References

- [1] H.Y. Shu, M.C. Chang, H.W. Hsu, Activated carbon supported iron–nickel bimetallic nanoparticles for decolorization of Reactive Black 5 wastewater, *Desalin. Water Treat.* 54 (2015) 1184–1193.
- [2] H.Y. Shu, M.C. Chang, Decolorization effects of six azo dyes by O_3 , UV/ O_3 and UV/ H_2O_2 processes, *Dyes Pigm.* 65 (2005) 25–31.
- [3] W. Baran, E. Adamek, A. Makowski, The influence of selected parameters on the photocatalytic degradation of azo-dyes in the presence of TiO_2 aqueous suspension, *Chem. Eng. J.* 145 (2008) 242–248.
- [4] W.A. Sadik, Effect of inorganic oxidants in photodecolourization of an azo dye, *J. Photochem. Photobiol. A-Chem.* 191 (2007) 132–137.
- [5] J.P. Guin, D.B. Naik, Y.K. Bhardwaj, L. Varshney, An insight into the effective advanced oxidation process for treatment of simulated textile dye waste water, *RSC Adv.* 4 (2014) 39941–39947.
- [6] B.H. Moon, Y.B. Park, S.S. Kim, G.T. Seo, T.S. Lee, T.S. Kim, Degradation of Azo dyes by the reduction and oxidation with nano sized zero valented iron, *Mater. Sci. Forum* 544–545 (2007) 705–708.
- [7] C.H. Wu, C.Y. Kuo, C.L. Chang, Decolorization of C.I. Reactive Red 2 by catalytic ozonation processes, *J. Hazard. Mater.* 153 (2008) 1052–1058.
- [8] N.K. Daud, B.H. Hameed, Decolorization of Acid Red 1 by Fenton-like process using rice husk ash-based catalyst, *J. Hazard. Mater.* 176 (2010) 938–944.
- [9] N. Daneshvar, M.H. Rasoulifard, A.R. Khataee, F. Hosseinzadeh, Removal of C.I. Acid Orange 7 from aqueous solution by UV irradiation in the presence of ZnO nanopowder, *J. Hazard. Mater.* 143 (2007) 95–101.
- [10] H. Katsumata, S. Koike, S. Kaneco, T. Suzuki, K. Ohta, Degradation of Reactive Yellow 86 with photo-Fenton process driven by solar light, *J. Environ. Sci.* 22 (2010) 1455–1461.
- [11] H. Kusic, I. Peternel, S. Ukic, N. Koprivanac, T. Bolanca, S. Papic, A.L. Bozic, Modeling of iron activated persulfate oxidation treating reactive azo dye in water matrix, *Chem. Eng. J.* 172 (2011) 109–121.

- [12] A. Khani, M.R. Sohrabi, M. Khosravi, M. Davallo, Enhancing purification of an azo dye solution in nano-sized zero-valent iron-ZnO photocatalyst system using subsequent semibatch packed-bed reactor, *Turk. J. Eng. Environ. Sci.* 37 (2013) 91–99.
- [13] H.Y. Shu, M.C. Chang, S.W. Huang, UV irradiation catalyzed persulfate advanced oxidation process for decolorization of Acid Blue 113 wastewater, *Desalin. Water Treat.* 54 (2015) 1013–1021.
- [14] S.F. Cheng, S.C. Wu, The enhancement methods for the degradation of TCE by zero-valent metals, *Chemosphere* 41 (2000) 1263–1270.
- [15] Y. Liu, F. Yang, P.L. Yue, G. Chen, Catalytic dechlorination of chlorophenols in water by palladium/iron, *Water Res.* 35 (2001) 1887–1890.
- [16] N. Kluyev, A. Cheleptchikov, E. Brodsky, V. Soyfer, V. Zhilnikov, Reductive dechlorination of polychlorinated dibenzo-p-dioxins by zerovalent iron in subcritical water, *Chemosphere* 46 (2002) 1293–1296.
- [17] M.C. Chang, H.Y. Shu, W.P. Hsieh, M.C. Wang, Using nanoscale zero-valent iron for the remediation of polycyclic aromatic hydrocarbons contaminated soil, *J. Air Waste Manage. Assoc.* 55 (2005) 1200–1207.
- [18] I.F. Cheng, R. Muftikian, Q. Fernando, N. Korte, Reduction of nitrate to ammonia by zero-valent iron, *Chemosphere* 35 (1997) 2689–2695.
- [19] Z. Xiong, D. Zhao, G. Pan, Rapid and complete destruction of perchlorate in water and ion-exchange brine using stabilized zero-valent iron nanoparticles, *Water Res.* 41 (2007) 3497–3505.
- [20] B. Geng, Z. Jin, T. Li, X. Qi, Kinetics of hexavalent chromium removal from water by chitosan-Fe⁰ nanoparticles, *Chemosphere* 75 (2009) 825–830.
- [21] J. Cao, L. Wei, Q. Huang, L. Wang, S. Han, Reducing degradation of azo dye by zero-valent iron in aqueous solution, *Chemosphere* 38 (1999) 565–571.
- [22] S. Nam, P.G. Tratnyek, Reduction of azo dyes with zero-valent iron, *Water Res.* 34 (2000) 1837–1845.
- [23] M.C. Chang, H.Y. Shu, H.H. Yu, Y.C. Sung, Reductive decolorization and total organic carbon reduction of the diazo dye CI Acid Black 24 by zero-valent iron powder, *J. Chem. Technol. Biotechnol.* 81 (2006) 1259–1266.
- [24] H.Y. Shu, M.C. Chang, H.H. Yu, W.H. Chen, Reduction of an azo dye Acid Black 24 solution using synthesized nanoscale zerovalent iron particles, *J. Colloid Interface Sci.* 314 (2007) 89–97.
- [25] H.Y. Shu, M.C. Chang, C.C. Chen, P.E. Chen, Using resin supported nano zero-valent iron particles for decoloration of Acid Blue 113 azo dye solution, *J. Hazard. Mater.* 184 (2010) 499–505.
- [26] W.X. Zhang, C.B. Wang, H.L. Lien, Treatment of chlorinated organic contaminants with nanoscale bimetallic particles, *Catal. Today* 40 (1998) 387–395.
- [27] R.J. Barnes, O. Riba, M.N. Gardner, T.B. Scott, S.A. Jackman, I.P. Thompson, Optimization of nano-scale nickel/iron particles for the reduction of high concentration chlorinated aliphatic hydrocarbon solutions, *Chemosphere* 79 (2010) 448–454.
- [28] A. Negroni, G. Zanaroli, M. Vignola, F. Fava, H.Y. Shu, Reductive dechlorination of polychlorinated biphenyls (PCBs) by means of nanoscale zero-valent nickel-iron (NZVNI) particles, *Environ. Eng. Manage. J.* 11 (2012) 1733–1739.
- [29] G. Zanaroli, A. Negroni, M. Vignola, A. Nuzzo, H.Y. Shu, F. Fava, Enhancement of microbial reductive dechlorination of polychlorinated biphenyls (PCBs) in a marine sediment by nanoscale zerovalent iron (NZVI) particles, *J. Chem. Technol. Biotechnol.* 87 (2012) 1246–1253.
- [30] Y. Mu, H.Q. Yu, S.J. Zhang, J.C. Zheng, Kinetics of reductive degradation of Orange II in aqueous solution by zero-valent iron, *J. Chem. Technol. Biotechnol.* 79 (2004) 1429–1431.